

**TURBULENT MIXING OF A CLOUD WITH THE
ENVIRONMENT: TWO-PHASE EVAPORATING FLOW.
NUMERICAL SIMULATIONS, LABORATORY EXPERIMENTS
AND FIELD MEASUREMENTS**

SZYMON P. MALINOWSKI

*University of Warsaw, Faculty of Physic, Poland
e-mail: mlina@fuw.edu.pl*

A brief overview of numerical simulations, laboratory experiments and in-situ measurements aimed at investigation of the cloud-clear air interfacial mixing, conducted in recent years at the Institute of Geophysics, University of Warsaw is presented. The most interesting finding from these studies is that the evaporative cooling at the interface separating cloudy and clear filaments results in density differences in scale of centimeters. This effect influences smallest scales of turbulent motions through production of TKE by buoyancy forces and makes the small-scale turbulence anisotropic.

Key words: two-phase flow, turbulent mixing, cloud interface

1. Introduction

While smallest scales of turbulence and turbulent mixing generated in controlled conditions (laboratory, wind tunnel) are widely discussed in the scientific literature (e.g. reviews by Sreenivasan and Antonia, 1997; Warhaft, 2000; Dimotakis, 2006), it is hard to find a single paper about in-situ measurements of the small-scale turbulence in clouds. By the "small-scale" we understand turbulence at the end of inertial range, i.e. at scales from 10cm down to the Kolmogorov microscale, which for typical atmospheric flows is a fraction of 1 mm.

Cloud turbulence extends beyond the range of that in laboratory flows ($Re \sim 10^8$ - 10^9 , $Re \sim 10^4$ - 10^5 , Siebert *et al.*, 2006), covering a range of scales from hundreds of meters down to a fraction of 1mm. In a cloud, we may expect a lot of intermittency, much more than in the lab. Making experiments in the lab, we know (almost) everything about the source of Turbulent Kinetic Energy (TKE), while performing measurements in the free atmosphere we usually

guess only about the origin of turbulence. A lot of potential sources of TKE are possible: shear instability, convective instability, gravity wave breaking, more specific sources due to moist thermodynamics and radiative cooling. In this paper, we focus on a particular source of the small-scale TKE in clouds: buoyancy production due to evaporation of cloud droplets. We investigate the interaction of small-scale turbulence with cloud microphysics and thermodynamics. The goal of the paper is to illustrate these effects stressing briefly results from laboratory and numerical experiments as well as in-situ measurements performed by the author and his collaborators. We wish to present to the reader some complex and interesting properties of processes which occur every day just above our heads. In the next Section we give a brief its information on cloud microphysics and its interaction with turbulence; in Section 3 we show how small-scale turbulent motion can be generated by evaporation of cloud droplets; in Sections 4-6 we present numerical, laboratory and in situ evidence that such a effect exists in nature. In Summary, we discuss possible consequences of presented features.

2. Thermodynamical reactions at the cloud-clear air interface and generation of motion from evaporation of cloud droplets

Consider a bubble of saturated air containing droplets of diameters of ca $10\ \mu\text{m}$ suspended in a still unsaturated environment. Remember, that the typical distance between droplets in a cloud is $\sim 1\ \text{mm}$, typical terminal fall velocity (Stokes regime) is $\sim 1\ \text{mm/s}$, and typical evaporation time of a small droplet is of the order of 1s (see e.g. Malinowski and Grabowski, 1997). Assume that the bubble has zero buoyancy (its mean density is the same as density of the environment) and its temperature is the same as of the environmental air. This is possible, since the density deficit due to humidity (virtual temperature effect) can be compensated by the Liquid Water Content (LWC). In terms of atmospheric thermodynamics, we state that the density temperature of the bubble is the same as the density temperature of the environment (see e.g. textbook by Emmanuel, 1994)

$$T_e \left(1 - \left(1 + \frac{R_v}{R_a} \right) x_e \right) = T_b \left(1 + \left(1 - \frac{R_v}{R_a} \right) X_b - w_b \right) \quad (2.1)$$

Here T denotes temperature, x is the water vapour mixing ratio (X denotes saturation), w is the liquid water mixing ratio, R_a and R_v stay for gas constants of dry air and water vapour, respectively. The index e denotes the environment, while the index b denotes the cloud bubble. L.h.s of equation

(2.1) represents density temperature of the unsaturated environment and the r.h.s. denotes that of the saturated cloud.

Notice, that term "density temperature" was introduced in order to facilitate understanding of the buoyancy term in the equation of motion. w can be a mixing ratio of any mater (liquid, aerosol) suspended in the mixture. This differs from the "virtual temperature" which is derived on the basis of a mixture of perfect gases.

In Fig. 1, an exemplary mixing diagram, showing the dependence of the density temperature of the mixture of the cloudy and environmental air on the proportion of mixing is presented. Values of thermodynamic parameters are representative for a typical summer small cumulus and satisfy our assumption of zero buoyancy of the cloud bubble. The diagram shows that evaporation of liquid water due to mixing with the unsaturated environment results in cooling. The mixture is more dense than the bubble and the environment. The maximum cooling effect in this particular example is for the mixing proportion of 40% of the environmental and 60% of the cloudy air.

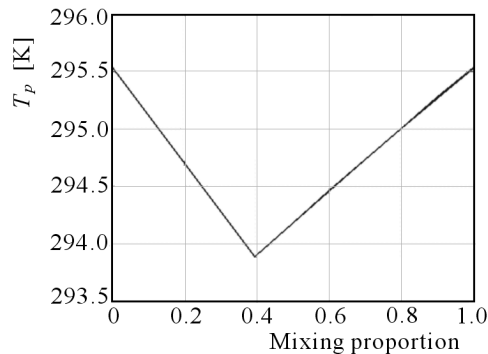


Fig. 1. Density temperature of a mixture of environmental air of temperature 20.5°C and relative humidity of 70% with saturated cloudy air of temperature 20.1°C and the liquid water mixing ratio 2 g/kg in function of proportion of the environmental air in the mixture

For a while we focus on the edge of the bubble. At its interface there is a jump of the water vapour mixing ratio: $X_b \neq x_e$. There is transport of water vapour across the cloud-clear air interface from the bubble interior to the environment due to molecular diffusion. Relative humidity in the vicinity of cloud droplets close to the interface decreases. Droplets evaporate cooling the interface. At the same moment, droplets fall due to gravity – they move with respect to the air. Below the cloud bubble they enter the unsaturated environment. This mechanism transports liquid water down which results in evaporation cooling the environment below the bubble. As a result of both processes a sheet of cool, dense air appears: thin at the sides of the bubble,

thicker below the cloud. Additionally, in the uppermost part of the bubble the density temperature increases, since droplets fall into the bubble interior leaving saturated, warm air at the top.

Density differences result in buoyancy forces, which initiate motion of the air. A complicated flow pattern appears in the initially still medium. Summarizing: the mechanism which produces buoyancy acts in the millimeter and centimeter scale in the region close to the interface. It is driven by transport of water vapour and liquid water across the interface and subsequent effects of evaporation.

3. Numerical simulations

The phenomena mentioned in the previous Section were investigated in a series of 3D numerical simulations with the use of EULAG model (Grabowski and Smolarkiewicz, 2002). Details of these simulations and full set of equations adopted are described in Andrejczuk *et al.* (2000, 2004, 2006). Briefly speaking, the Navier-Stokes equations in the Boussinesq approximation together with equations for thermodynamics and microphysics are solved. Thermodynamics equations account for phase changes (evaporation/condensation) while microphysics in most simulations is parameterized with 16/32 classes of droplets which move with respect to the air with the terminal velocity depending on the droplet radius in each class. In Section 3.2, an additional simplified run with bulk parameterization of thermodynamics/microphysics is also described. Bulk parameterization accounts for the phase change/latent heat effects, but does not account for the motion of droplets.

Simulations were performed in a volume of approximately $0.6 \times 0.6 \times 0.6$ m at 1 cm, 0.5 cm and 0.25 cm resolutions (64^3 to 256^3 gridboxes). Cyclic boundary conditions in all directions were chosen. The gridbox size is a compromise between full DNS resolving the smallest scales of motion and microphysics parameterization, in which each class of droplets is represented by a continuous field. Arguments supporting such an approach, called sometimes "poorly resolved DNS" or "underresolved DNS", can be found in Margolin *et al.* (2006).

3.1. Experiments with zero-buoyancy bubble in still air

In Fig. 2, results of exemplary simulation with the hypothetical cloudy bubble described in the previous Section are shown. In three panels, there are vertical cross-sections through the bubble after 11 seconds of simulations. The isolines mark concentration of the passive scalar put inside the bubble in the beginning of simulations in order to indicate diffusion in the model

volume. In Fig. 2a, the field of liquid water content is presented. It is clear that sedimentation of droplets result in separation of the air in the bubble and liquid water. The cooling due to evaporation of droplets is shown in Fig. 2b in terms of the density temperature. Notice the dark pattern indicating the cool area in the bottom part of the bubble. This cooling causes sinking motion, indicated in Fig. 2c with the vertical velocity field.

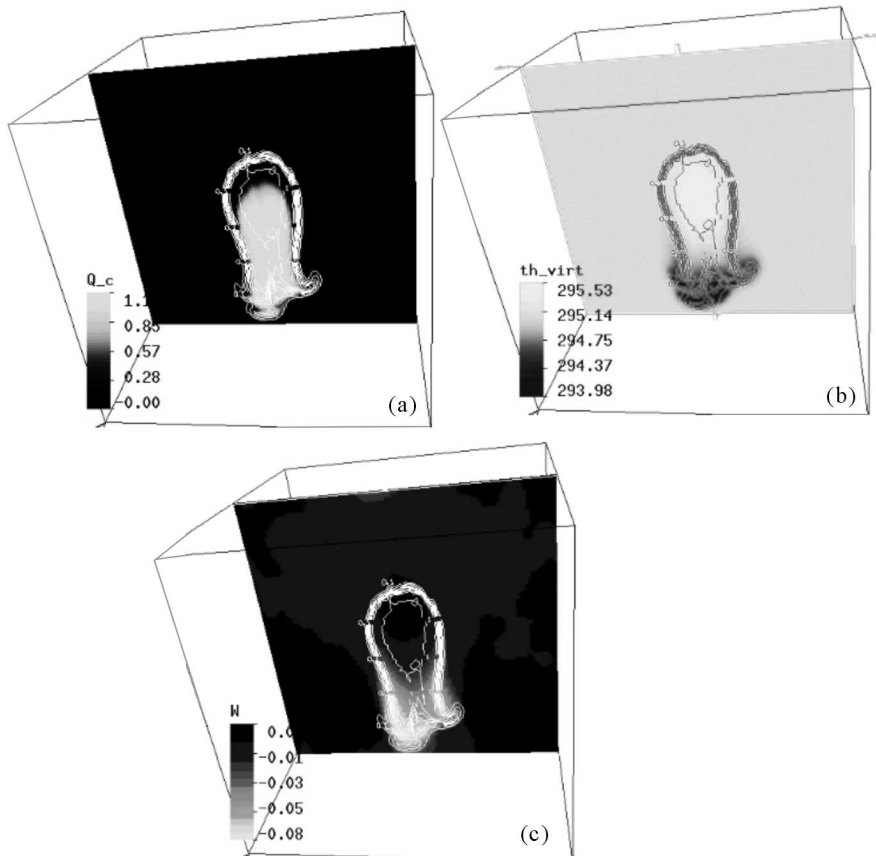


Fig. 2. Numerical simulations of the evolution of neutrally buoyant cloudy bubble (density temperature as in Fig. 1) in unsaturated environment. Liquid water content in g/kg (a), temperature density in K (b) and vertical velocity in cm/s (c) fields on the vertical cross-section through the computational domain after 11s of simulations

3.2. Simulations with mixing

In Fig. 3, a snapshot from different simulations is presented. The simulations were designed to show fine details of the turbulent mixing at the edge of the cloud. In contrary to the previous case, the simulations were initiated with

the prescribed velocity field, aimed to mimic final stages of the slow turbulent mixing between the cloud and the environment at scales of tens of cm (for the details see Andrejczuk *et al.*, 2004, 2006). The particular pattern was taken after Herring and Kerr (1996), who simulated decaying turbulence. The initial interface between the cloud and the environment was convoluted according to the same rule. Vertical and horizontal cross-sections through the computational domain after 11 s of simulations are shown in Fig. 3. Cloudy filaments of brightness proportional to the liquid water mixing ratio are intertwined with clear air (no liquid water) filaments.

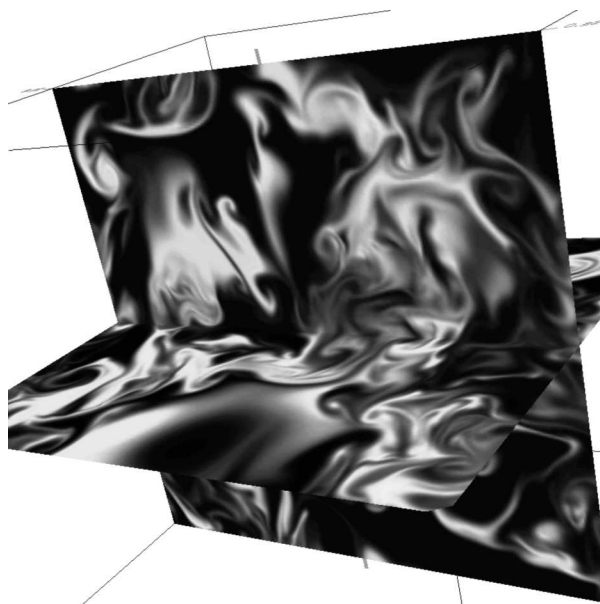


Fig. 3. Nearly DNS (2.5 mm spatial resolution) numerical simulation of a mixing event at the cloud-clear air interface. Vertical and horizontal cross-sections through the computational domain after 11 s of simulations reveal liquid water content filaments (bright patterns) intertwined with clear air filaments

In Fig. 4 evolution of the average (mean over the whole computational domain) Turbulent Kinetic Energy (TKE) in course of such simulations is presented. There are two curves: dashed showing TKE in course of the simulation with the detailed microphysics, and solid presenting TKE in simulation with the bulk microphysics. In both cases, we see that the initial TKE increases in the first 9-10 s of simulations. At this period, the interface separating cloudy and clear air filaments increases and generation of TKE due to effects described in Section 2 dominates the motion. After 9-10 s of simulations the generation becomes weaker, growing dissipation compensates and later dominates the TKE evolution. Calculations were stopped after 25 s of simulations, when the volume became almost homogeneous in terms of thermodynamics and

microphysics. Comparison of runs with different parameterizations of microphysics clearly indicates the role of water transport from the cloudy filaments to unsaturated clear air due to droplet sedimentation.

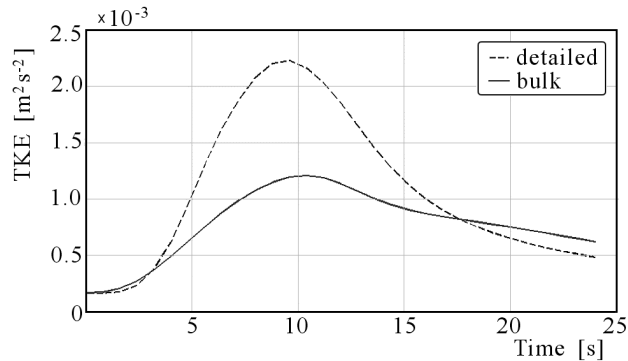


Fig. 4. Evolution of TKE in simulations of the mixing event at the cloud-clear air interface. Initially small turbulent kinetic energy transported down from large scales is increased due to buoyancy forces generated at the cloud clear air interface by evaporative cooling of cloud droplets. After 10s generation of TKE slows down and dissipation increases resulting in TKE decay. The dashed line represents simulation with detailed microphysics accounting for droplet sedimentation from cloudy to clear air filaments, while the continuous line represents simulation with bulk microphysics, in which only phase changes were accounted

Consider that in the investigated cases, TKE is produced in course of mixing due to the action of buoyancy forces. These forces act in the vertical direction, i.e. production of TKE in small-scales is anisotropic, suggesting anisotropy of small-scale turbulence with the preferred vertical direction. Statistical properties of turbulent velocity fluctuations documenting this feature are summarized in Table 1.

Table 1. Distribution of horizontal (u' , v') and vertical (w') turbulent velocity fluctuations after 15 s of calculations

	Standard deviation [cm/s]	Skewness	Kurtosis
u'	3.19	-0.07	3.3
v'	3.09	-0.13	3.3
w'	4.56	0.15	3.0

4. Laboratory experiments with cloud-clear air mixing

Classical laboratory experiments with stirring of fluids (Broadwell and Breidenthal, 1982) and turbulent mixing (Sreenivasan *et al.*, 1989) were adopted to construct conceptual models of cloud-clear air mixing (Baker and Latham, 1984; Malinowski and Zawadzki, 1993). More recent experiments: visualization by the laser sheet photography of turbulent mixing of cloud and clear air (Malinowski *et al.*, 1998) provide insights into the cloud structure at small scales.

4.1. Geometry of small-scale patterns

Analysis of the images obtained in experiments indicates that the small-scale patterns created in course of mixing have different similarity properties in scales above 2 cm and below 2 cm (Banat and Malinowski, 1999). The interface separating cloudy and clear air filaments is convoluted. Patterns at scales larger than 2 cm are self-similar, resembling the isoconcentration surfaces of passive scalars (see e.g. Sreenivasan *et al.*, 1989). At scales smaller than 2 cm there is no self-similarity and interfaces can be described in terms of geometrical surfaces. Filaments created in the process of mixing are anisotropic with the preferred vertical direction, indicating the importance of buoyancy forces, which stretch the filaments in vertical.

The "thickness" of the cloud-clear air interface depends on its orientation in space (Malinowski and Jaczewski, 1999). Horizontal interfaces are less sharp than vertical ones indicating that the droplet sedimentation plays an important role. These conclusions served as motivation to numerical experiments discussed in the previous Section and helped to design new experiments.

4.2. Dynamics of mixing analysed with the particle imaging velocimetry

An improved visualization technique allowed for investigation of mixing by means of the Particle Imaging Velocimetry (PIV) approach. A detailed description of the experiments can be found in Korczyk *et al.* (2004, 2006) and a short analysis of recent results in Malinowski *et al.* (2006). In brief, we investigated the cloud-clear air mixing observing motion of cloud droplets in a glass walled chamber 1m deep, 1m wide and 1.8 m high. The second smaller chamber placed above the main one was filled with saturated air containing water droplets of diameters in range from 7 to 25 μm , similar to those in real clouds. After opening the hole between the chambers, this air began to descend forming a negatively buoyant, turbulent plume undergoing mixing with the unsaturated air in the main chamber. The plume was illuminated with

a 1.2 mm wide sheet of laser light (Nd:YAG, $\lambda = 532$ nm) forming a vertical cross-section through the central part of the chamber. Images, formed due to Mie scattering of the laser light by cloud droplets were recorded by a high-resolution CCD camera placed outside the chamber with the optical axis perpendicular to the light sheet. The images were recorded in pairs in order to retrieve information on droplets velocities. Application of standard PIV algorithms to these pairs resulted in a large amount of errors and artifacts in the retrieved velocity field due to chaotic nature of motion in the chamber. Therefore, a special multi-scale algorithm was developed (Korczyk *et al.*, 2006).

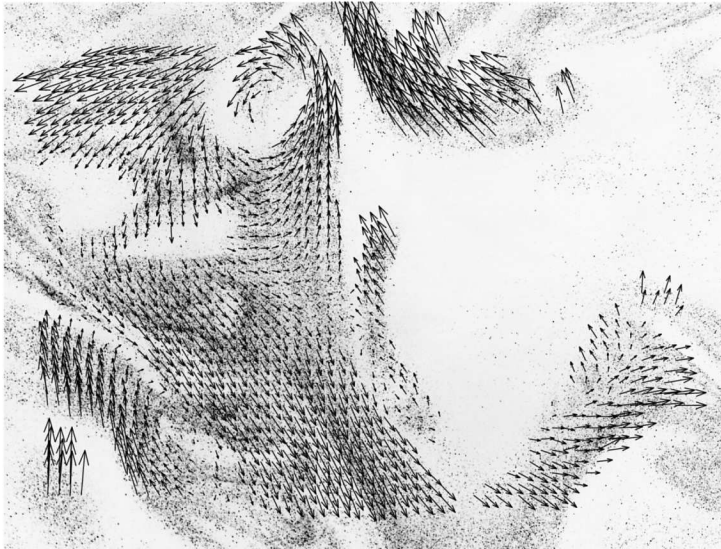


Fig. 5. Cloud-clear air mixing observed with the laser sheet technique in a cloud chamber. Vectors represent the retrieved information on velocity of cloud droplets in the plane of the light sheet with the use of Particle Imaging Velocimetry (PIV technique)

An exemplary image with superimposed vectors of the 2D velocity field is presented in Fig. 5. Notice that the PIV technique allows one to reconstruct the field of motion of droplets, not the air itself. Since the droplets are present only in cloudy filaments, we have no information of the flow in clear air volumes. A short discussion of the influence of these limitations on the resulting velocity field as well as preliminary results from these experiments are given in Korczyk *et al.* (2006). Owing to these results, we summarize statistical properties of horizontal and vertical velocity fluctuations from 19 scenes from the chamber (Table 2). Notice, that values of standard deviations differ from that in Table 1 (numerical experiments) due to the difference in environmental

conditions, while higher order moments mostly agree. Notice also that in both cases standard deviations in the vertical direction are ~ 1.5 times greater than those in the horizontal one, indicating anisotropy with the preferred vertical direction.

Table 2. Distribution of horizontal (u') and vertical (w') turbulent velocity fluctuations in the experiment

	Standard deviation [cm/s]	Skewness	Kurtosis
u'	5.4	-0.01	3.2
w'	8.0	-0.20	3.1

5. In-situ measurements

Direct measurements in clouds at scales as small as in the laboratory and numerical experiments discussed above are beyond our instrumental capabilities. Nevertheless, with the use of the available experimental data we may argue that the above presented laboratory and numerical results close the unexplored in nature gap at the high resolution end of the spectrum. The best airborne systems resolve velocity fluctuation down to a fraction of meter (Siebert *et al.*, 2006). At these scales, the anisotropy of turbulent fluctuations of velocity has not been experimentally confirmed. Notice, however, that TKE in scales of tens of cm comes from the transport of TKE from larger scales down in the cascade process. Since in 3D turbulence there is no transport toward larger scales, there is no way to argue whether small-scale processes influence the turbulence below the resolution range.

Several instruments allow for investigation of thermodynamical and microphysical properties of cloud-clear air mixing down to ~ 10 cm resolution and less. These are Ultra-Fast Thermometer (UFT, Haman *et al.*, 1997, 2003), Particle Volume Meter (PVM, Gerber *et al.*, 1994) and Fast-Forward Scattering Spectrometer Probe (F-FSSP Brenguier *et al.*, 1998). The best available data, showing the small-scale structure of clouds inferred from measurements with the use of these sensors mounted on an aircraft, were collected during the DYCOMS-II experiment (Stevens *et al.*, 2003). Some of the data were presented by Haman *et al.* (2007). Convolutated patterns created in course of the mixing of a cloud with the environment with filaments as narrow as 10 cm resemble patterns observed during numerical experiments and in the lab.

In order to facilitate the reader with the high-resolution aircraft data, which are 1D sections through the sampling volume, we show an example of a

temperature record collected with the UFT sensor at the edge of a Cumulus cloud (Fig. 6). The spatial resolution between the samples resulting from the data acquisition rate (10 kHz) and aircraft velocity (70 m/s) in this particular case was 0.7 cm. Accounting for low-pass filtering in the recording system, we state that thermal structures of scales more than 5 cm are recorded without significant distortions.

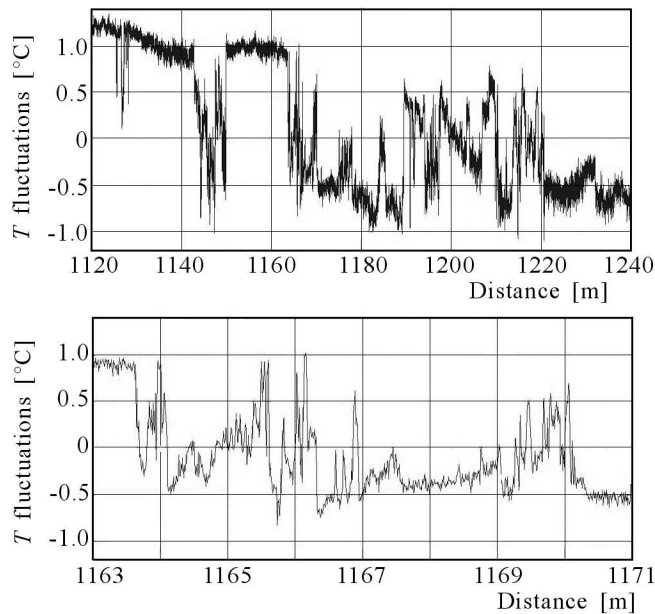


Fig. 6. High resolution (7 mm distance between the samples) data on temperature fluctuations at the cloud-clear air interface collected a board an aircraft with the UFT thermometer. In the upper panel a 120 m long record is shown. The blown-up segment (notice the range of the record) shows a fine structure of the temperature field due to filamentation during the process of mixing

Inspection of Fig. 6 indicates that the sensor passed through volumes of different temperatures separated by narrow interfaces. We infer that the air in these volumes origins from two distinct sources: the core of the cloud and the cloud environment as well as filaments of various sizes created during the mixing – see the upper panel in Fig. 6. The lower panel with a blown-up 8 m long segment shows filaments of order of 10 cm and less, which is close to the resolution of the sensor. Such a picture is characteristic for ongoing turbulent mixing of a cloud and the environment. Similar filamented structures of the cloud edge were reported in many papers (e.g. Baker, 1993; Davis *et al.*, 1999; Malinowski and Zawadzki, 1993; and many others). Presence of small filaments allows one to argue that the phenomena observed in the laboratory

and modelled with numerical simulations exist in real clouds, and that an effort to measure the anisotropy of turbulence in clouds should be undertaken.

6. Discussion and conclusions

In previous Sections, we have shown that the complicated interaction between dynamics, thermodynamics and microphysics influences the smallest scales of turbulence at the cloud-clear air interface. Evaporative cooling of cloud droplets at the cloud-clear air interface generates Turbulent Kinetic Energy in scales of centimeters and millimeters. The sedimentation of droplets is important for this process. Generation of buoyancy during cloud-clear air mixing causes makes the smallest scales of turbulence anisotropic.

While these effects have not been documented in natural conditions in free atmosphere due to insufficient experimental capabilities of current atmospheric science, their evidence has been confirmed by numerical simulations and laboratory experiments. Available in-situ data, showing string filamentation of the cloud-clear air interface support the hypothesis that such an effect may exist in nature.

Figure 4, showing generation of TKE in small scales due to evaporative cooling suggests that close to cloud edges the small-scale turbulence is stronger than expected from the available larger scale measurements. It seems also that it is anisotropic with the privileged vertical direction. These findings can be potentially important for unresolved problems of warm rain formation (Shaw, 2003; Vaillancourt and Yau, 2000), where collisions of droplets in small-scale turbulence have been identified as a mechanism leading to formation of participation particles.

Acknowledgments

Author thanks all collaborators from the Institute of Geophysics Warsaw University, Institute of Fundamental Technological Research Polish Academy of Sciences, Los Alamos National Laboratory and National Center for Atmospheric Research. Particular acknowledgments should be given to Mirosław Andrejczuk, Piotr Banat, Wojciech Grabowski, Krzysztof Haman, Adam Jaczewski, Piotr Korczyk, Tomasz Kowalewski, Marcin Kurowski and Piotr Smolarkiewicz. The research was supported by the Polish State Committee for Scientific Research, Polish Ministry of Science and Higher Education, by the US National Science Foundation, by NCAR's Clouds in Climate and Geophysical Turbulence programs as well as by the European grant EVK2-CT2002-80010-CESSAR. Computations were performed at the Interdisciplinary Center for Mathematical and Computational Modeling of Warsaw University and at the National Center for Atmospheric Research, Boulder, CO, USA.

References

1. ANDREJCZUK M., GRABOWSKI W.W., MALINOWSKI S.P., SMOLARKIEWICZ P.K., 2000, Numerical investigation of turbulent mixing of clouds with clear air in small scales: interactions of turbulence and microphysics, *Proceedings of 13th Conference on Clouds and Precipitation, IAMAP, Reno, Nevada, USA, 14-18 August 2000*, 152-154
2. ANDREJCZUK M., GRABOWSKI W.W., MALINOWSKI S.P., SMOLARKIEWICZ P.K., 2004, Numerical simulation of cloud-clear air interfacial mixing, *J. Atmos. Sci.*, **61**, 1726-1739
3. ANDREJCZUK M., GRABOWSKI W.W., MALINOWSKI S.P., SMOLARKIEWICZ P.K., 2006, Numerical simulation of cloud-clear air interfacial mixing: effects on cloud-microphysics, *J. Atmos. Sci.*, **63**, 3204-3225.
4. BAKER M.B., BREIDENTHAL R.E., CHOULARTON T.W., LATHAM J., 1984, The effects of turbulent mixing in clouds, *J. Atmos. Sci.*, **41**, 299-304
5. BANAT P., MALINOWSKI S.P., 1999, Properties of the turbulent cloud-clear air interface observed in the laboratory experiment, *Phys. Chem. Earth (B)*, **24**, 741-745
6. BRENGUIER J.-L., BOURRIANNE T., DE COELHO A.A., ISBERT J., PEYTAVI R., TREVARIN D., WESCHLER P., 1998, Improvements of droplet size distribution measurements with the Fast-FSSP (Forward Scattering Spectrometer Probe), *J. Atmos. Ocean. Technol.*, **15**, 1077-1090
7. BROADWELL J.E., BREIDENTHAL R.E., 1982, A simple model of mixing and chemical reaction in a turbulent shear layer, *J. Fluid. Mech.*, **125**, 397-410
8. DAVIS A., MARSHAK A., GERBER H., WISCOMBE W., 1999, Horizontal structure of marine boundary layer clouds from cm to km scales, *J. Geoph. Res.*, **104**, (D6), 6123-6144
9. DIMOTAKIS P.E., 2006, Turbulent mixing, *Ann. Rev. Fluid. Mech.*, **37**, 329-356
10. EMANUEL K.A., 1994, *Atmospheric Convection*, Oxford University Press, 580 p.
11. GERBER H., ARENDS B.G., ACKERMAN A.S., 1994, New microphysics sensor for aircraft use, *Atmos. Res.*, **31**, 235-252
12. GRABOWSKI W.W., SMOLARKIEWICZ P.K., 2002, A multiscale model for meteorological research, *Mon. Wea. Rev.*, **130**, 939-956
13. HAMAN K.E., MALINOWSKI S.P., 1996, Temperature measurements in clouds on a centimetre scale – preliminary results, *Atmos. Res.*, **41**, 161-175
14. HAMAN K.E., MAKULSKI A., MALINOWSKI S.P., BUSEN R., 1997, A new ultrafast thermometer for airborne measurements in clouds, *J. Atmos. Oceanic Technol.*, **14**, 217-227

15. HAMAN K.E., MALINOWSKI S.P., STRUŚ B.D., BUSEN R., STEFKO A., 2001, Two new types of ultrafast aircraft thermometers, *J. Atmos. Ocean. Technol.*, **18**, 117-134
16. HAMAN K.E., MALINOWSKI S.P., KUROWSKI M., GERBER H., BRENGUIER J.-L., 2007, Small scale mixing processes at the top of a marine stratocumulus – a case study., *Q. J. Roy. Meteorol. Soc.*, **133**, 213-226
17. HERRING J.R., KERR R.M., 1993, Development of enstrophy and spectra in numerical turbulence, *Phys. Fluids A*, **5**, 11, 2792-2798
18. KORCZYK P.M., MALINOWSKI S.P., KOWALEWSKI T.A., 2004, Particle Image Velocimetry (PIV) for Cloud Droplets – Laboratory Investigations, *Abstracts Book and CD-ROM Proceedings, 21st International Congress of Theoretical and Applied Mechanics, August 15-21, Warsaw, Poland*, (cd-rom)
19. KORCZYK P.M., MALINOWSKI S.P., KOWALEWSKI T.A., 2006, Mixing of cloud and clear air in centimeter scales observed in laboratory by means of particle image velocimetry, *Atmos. Res.*, **82**, 173-182
20. MALINOWSKI S.P., ZAWADZKI I., 1993, On the surface of clouds, *J. Atmos. Sci.*, **50**, 5-13
21. MALINOWSKI S.P., GRABOWSKI W.W., 1997, Local increase in concentration of cloud droplets and water content resulting from turbulent mixing, *Journal of Technical Physics*, **38**, 397-406
22. MALINOWSKI S.P., ZAWADZKI I., BANAT P., 1998, Laboratory observations of cloud clear air mixing in small scales, *J. Atmos. Oceanic Technol.*, **15**, 1060-1065
23. MALINOWSKI S.P., JACZEWSKI A., 1999, Laboratory investigation of droplet concentration at the cloud-clear interface, *Phys. Chem. Earth (B)*, **24**, 477-480
24. MARGOLIN L.G., SMOLARKIEWLWCZ P.K., WYSZOGRAZDKI A.A., 2006, Dissipation in implicit turbulence models: a computational study, *Journal of Applied Mechanics, Transactions ASME*, **73**, 3, 469-473
25. SHAW R.A., 2003, Particle-turbulence interactions in atmospheric clouds, *Ann. Rev. Fluid Mech.*, **35**, 183-227
26. SIEBERT H., LEHMANN K., WENDISCH M., 2006, Observations of small-scale turbulence and energy dissipation rates in the cloudy boundary layer, *J. Atmos. Sci.*, **63**, 1451-1466
27. SREENIVASAN K.R., RAMSHANKAR R., MENEVEAU C., 1989, Mixing, entrainment and fractal dimension of surfaces in turbulent flow, *Proc. R. Soc. London A*, **421**, 79-108
28. SREENIVASAN K.R., ANTONIA R.A., 1997, The phenomenology of small-scale turbulence, *Ann. Rev. Fluid Mech.*, **29**, 435-472

29. STEVENS B., LENSCHOW D.H., VALI G., GERBER H., BANDY A., BLOMQUIST B., BRENGUIER J.-L., BRETHERTON C.S., BURNET F., CAMPOS T., CHAI S., FALOONA I., FRIESEN D., HAIMOV S., LAURSEN K., LILLY D. K., LOEHRER S.M., MALINOWSKI S.P., MORLEY B., PETERS M. D., ROGERS D. C., RUSSELL L., SAVIC-JOVICIC V., SNIDER J. R., STRAUB D., SZUMOWSKI, M.J., TAKAGI H., THORNTON D.C., TSCHUDI M., TWOHY C., WETZEL M., VAN ZANTEN M.C., 2003, Dynamics and chemistry of marine stratocumulus – Dycoms-II, *Bull. Amer. Meteorol. Soc.*, **84**, 579-593
30. VAILLANCOURT P.A., YAU M.K., 2000, Review of particle-turbulence interactions and consequences for cloud physics, *Bull. Amer Meteorol. Soc.*, **81**, 2, 285-298
31. WARHAFT Z., 2000, Passive scalars in turbulent flows, *Ann. Rev. Fluid Mech.*, **32**, 203-240

Turbulencyjne mieszanie chmury z otoczeniem jako przepływ dwufazowy z parowaniem. Symulacje numeryczne, eksperymenty laboratoryjne i pomiary *in situ*

Streszczenie

W artykule zawarto zwarty przegląd symulacji numerycznych, eksperymentów prowadzonych w laboratorium oraz pomiarów *in situ*, których celem było badanie mieszania turbulencyjnego na granicy chmury z nienasyconym otoczeniem. Badania te prowadzono w Instytucie Geofizyki Uniwersytetu Warszawskiego. Najciekawszym wynikiem tych prac jest pokazanie wpływu, jaki ma parowanie wody chmurowej na granicy chmury na dynamikę turbulencji w małych skalach. Parowanie powoduje powstanie lokalnych różnic gęstości o skali przestrzennej rzędu centymetrów. Działanie sił wyporu prowadzi do produkcji drobnoskalowej turbulencji. Ponieważ wyróżniony jest kierunek pionowy, turbulencja ta jest anizotropowa.

Manuscript received March 19, 2007; accepted for print May 23, 2007